Tuning the dimensionality of organometallic-organic hybrid polymers assembled from $[Cp_2Mo_2(CO)_4(\eta^2\text{-}P_2)]$, rigid bipyridyl linkers and Ag^I ions

Mehdi Elsayed Moussa,[a] Eugenia Peresypkina,[b,c] Alexander V. Virovets,[b,c] Dominik Venus,[a] Gábor Balázs[a] and Manfred Scheer*[a]

The reactions of the P_2 ligand complex $[Cp_2Mo_2(CO)_4(\eta^2\text{-}P_2)]$ (Cp = C_5H_5, 1) WITH $Ag[Al\{OC(CF_3)_3\}_4]$ (AG[TEF]) in the presence of the rigid bipyridyl linkers 1,2-di(pyridin-4-yl)ethyne (3), 4,4'-bis(pyridin-4-ylethynyl)-1,1'-biphenyl (4) and 4,4'-bipyridine (5) possessing various lengths are studied. The reaction with the longer linkers (3 and 4) leads TO THE FORMATION OF the 1D organometallic-organic hybrid polymers $[\{Cp_2Mo_2(CO)_4(\mu_4,\eta^{1:1:2:2}\text{-}P_2)\}_2\{Cp_2Mo_2(CO)_4(\mu_3,\eta^{1:2:2}\text{-}P_2)\}_2(\mu,\eta^{1:1}\text{-}C_{12}H_8N_2)Ag_2]_n[TEF]_{2n}$ (6) and $[\{Cp_2Mo_2(CO)_4\text{-}(\mu_4,\eta^{1:1:2:2}\text{-}P_2)\}_2\{Cp_2Mo_2(CO)_4(\mu_3,\eta^{1:2:2}\text{-}P_2)\}_2(\mu,\eta^{1:1}\text{-}C_{26}H_{16}N_2)Ag_2]_n[TEF]_{2n}$ (7) in high selectivity. A similar reaction with the short linker 5 affords a mixture of the 2D hybrid polymers $[\{Cp_2Mo_2(CO)_4(\mu_4,\eta^{1:2:2:2}\text{-}P_2)\}_2(\mu,\eta^{1:1}\text{-}C_{13}H_{14}N_2)Ag_2]_n[TEF]_{2n}$ (8) and the 3D hybrid network $[\{(Cp_2Mo_2(CO)_4(\mu_4,\eta^{1:1:2:2}\text{-}P_2)\}_2(\mu,\eta^{1:1}\text{-}C_{10}H_8N_2)Ag]_n[TEF]_{2n}$ (9). However, a selective synthesis of 8 or 9 is possible when the reaction is performed at 0°C and 60°C, RESPECTIVELY.

Over the last few decades, the field of coordination polymers (CPs) has attracted great attention due to their fascinating topologies and potential applications as functional materials.[1] Until recently, these compounds have commonly been assembled via the coordination of tailor-made multitopic organic linkers (bearing usually N-, O-, or S-donor atoms) to transition metal ions.[2] However, it is highly challenging to attain selectivity using this synthetic approach as the assembling reactions are influenced by many factors including the used solvent mixture, counterion, the nature of the organic linker, the reaction temperature and many others.[1g,3] To avoid the low selectivity of the mentioned reactions, chemists have developed several alternative methods.[4,5] One of these methods relies on the use of rigid organic ligands, as these molecules do not possess conformational freedom, which is why they support, to some extent, the formation of one thermodynamically stable product.[5] In contrast to other approaches in this field, our group is interested in using polyphosphorus and polyarsenic ligand complexes with flexible coordination modes as organometallic connecters between metal ions, a novel approach allowing the synthesis of 1D, 2D, and 3D CPs,[6] nano-sized fullerene-like supramolecular spheres,[7] and molecular organometallic capsules.[8] More recently, a variety of these ligand complexes (e.g. $[Cp_2Mo_2(CO)_4(\eta^2\text{-}P_2)]$ (**1**)), were reacted in three-component reactions with Ag^I and Cu^I salts in the presence of N-based ditopic linkers to give unprecedented organometallic-organic hybrid CPs.[9] Based on these results, we became further interested in tuning the dimensionality of the formed hybrid polymers using various reaction conditions. The main challenge lies in the understanding of the proceeding pathway to direct the synthesis of organometallic-organic MOF-like networks and obtain selectively 2D or 3D hybrid materials.

Herein, we report the effect of the length of the organic linker and the reaction temperature on assemblies obtained from the reaction of the ligand complex **1**, $Ag[Al\{OC(CF_3)_3\}_4]$ **(AG[TEF])** and ditopic pyridine-based linkers **3**-**5**. Using the short linker 4,4'-bipyridine (**5**) instead of the longer linkers 1,2-di(pyridin-4-yl)ethyne (**3**) or 4,4'-bis(pyridin-4-ylethynyl)-1,1'-biphenyl (**4**) afforded (at room temperature) totally different results, as 1D hybrid CPs are formed (by using **3** or **4**) instead of a mixture of 2D and 3D hybrid CPs (by using **5**). In addition, we realized for the first time that these 2D and 3D CPs can each be selectively obtained depending on the reaction temperature. The formation of these products together at room temperature and their selective formation at low (0°C, **8**) and high (60°C, **9**) temperatures are studied experimentally and modelled by DFT calculations. Although these two factors (the organic linker length and the reaction temperature) were studied in literature for CPs and MOFs,[3] to the best of our knowledge, this is the first study of these factors in the field of organometallic-organic hybrid polymers.

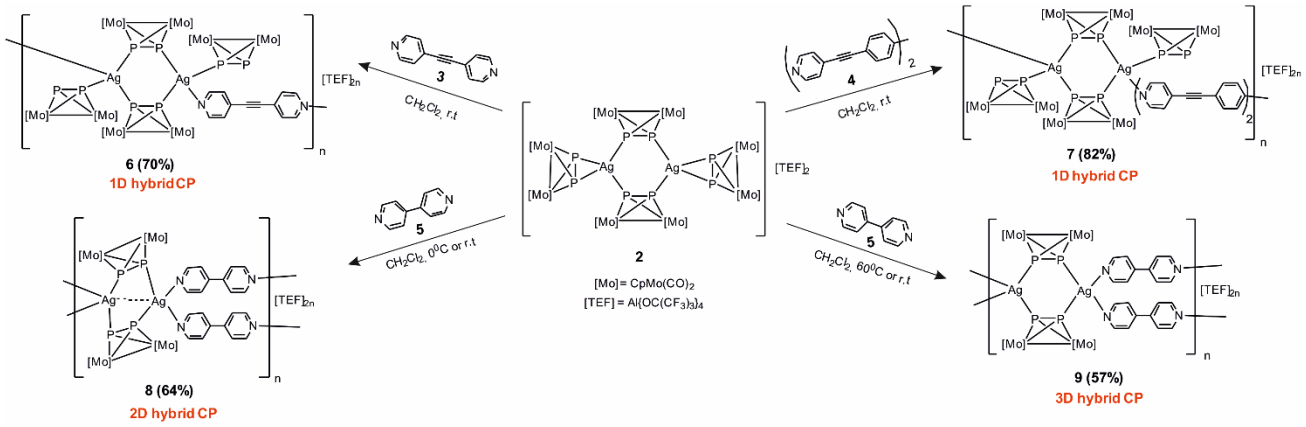

Scheme 1. Summary of the reaction of the Ag^{I} dimer **2** with the dipyridyl linkers **3**-**5** to give the organometallic-organic hybrid CPs **6**-**9**.

Recently,[6a] we have reported that the reaction of the P_2 ligand complex $[Cp_2Mo_2(CO)_4(\eta^2\text{-}P_2)]$ (**1**) with Ag[TEF] allows the synthesis of the Ag^{I} dimer **2** (Scheme 1). In the solid state, this dimer is stabilized by four ligands **1** with two of them adopting a $\mu\text{-}\eta^1\text{:}\eta^1$ coordination mode and the other two being η^2-coordinated. Now, in a first step, the dimer **2** was reacted with the ditopic pyridine-based linkers **3** or **4**. These reactions were performed in a 1:1 stoichiometry at room temperature in CH_2Cl_2 and led to the selective formation of the compounds **6** or **7** as orange crystalline solids suitable for single crystal X-ray structure analysis (Scheme 1). In each case, the same product could also be selectively isolated by mixing together the simple components complex **1**, Ag[TEF] and the linkers **3** or **4** in a one-pot reaction using 1, 2 or 3 equivalents of the organic linkers, which suggests that the products (**6** and **7**) are thermodynamically favored and easily reproducible. The X-ray structure analysis performed for **6** and **7** reveals that they are 1D organometallic-organic hybrid CPs consisting of $[Ag_2(\mathbf{1})_4]$

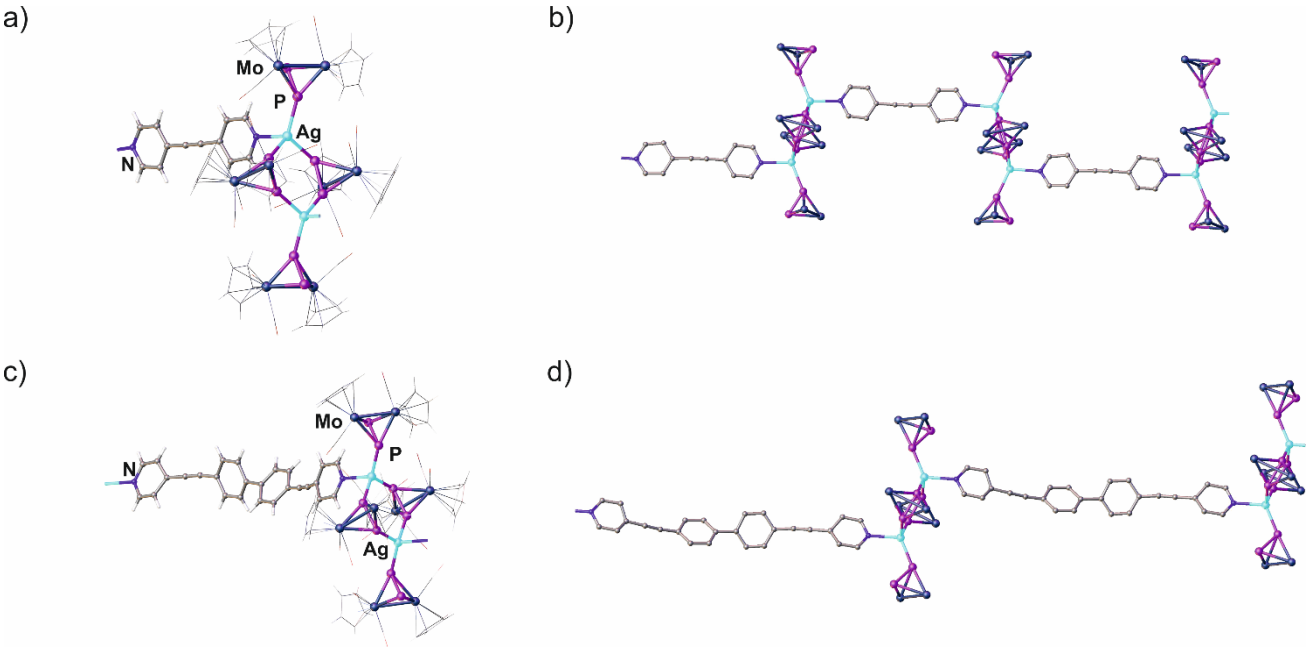

Figure 1. The dicationic repeating units of a) **6** and c) **7** and the corresponding sections of the 1D hybrid polymers b) **6** and d) **7** in the solid state. Cp, CO ligands, H atoms, counteranions and minor positions of disordered fragments are omitted for clarity.

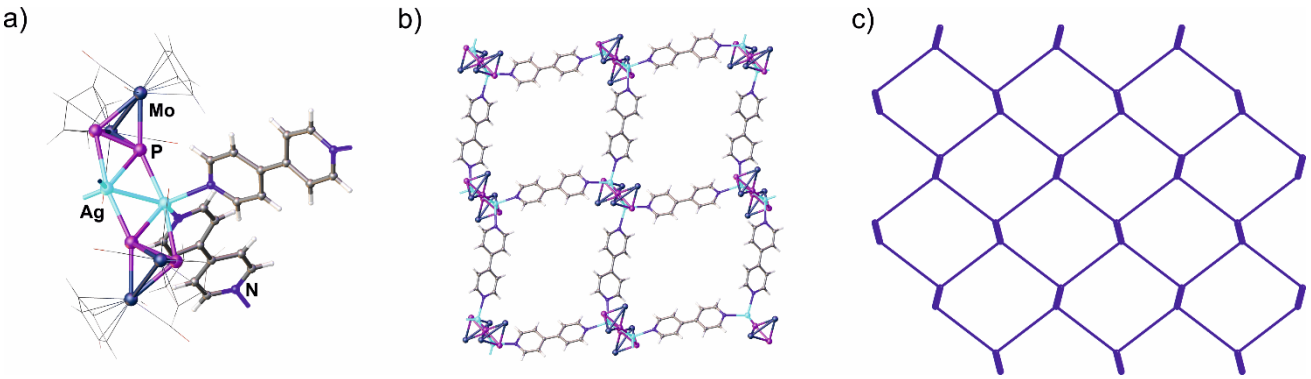

Figure 2. a) The dicationic repeating unit of **8** and b) Section of the 2D hybrid polymer **8** in the solid state. Cp and CO ligands are omitted for clarity. c) Simplified view of the layer of **hcb** topology formed by silver nodes as well as Mo_2P_2 and bipyridyl ligands as linkers in **8**.[12,13] (organic linkers depicted as long rods and the $Ag_2P_2(MoCp(CO)_2)_2$ moieties as thick cylinders).

units, which are linked together by the connectors **3** and **4**, respectively (Figure 1). The coordination mode of the formerly η^2-coordinating ligand complexes **1** in the Ag^I dimer **2** turned into a η^1-coordination, which enabled the coordination of the organic linker molecules. Nevertheless, the Ag_2P_4 six-membered ring motif of **2** is conserved in the structures of **6** and **7**. These six-membered rings are almost planar in **6** (folding angle: 5.0(4)°), whereas they show a pronounced chair conformation in **7** (folding angle: 39.0(2)°). The Ag^I ions in both polymers comprise distorted tetrahedral environments possessing three P atoms and one N atom. The P-P bond lengths in **6** (2.078(8)-2.091(7) Å) and **7** (2.08(2)-2.20(2) Å) are on average slightly elongated compared to the free complex **1** (2.079(6) Å).[10] The Ag-P bond lengths in **6** (2.471(6)-2.512(5) Å) and **7** (2.313(1)-2.624(1) Å) are in the typical range and comparable to those of the dimer **2** (2.463(4)-2.688(5) Å).[6a] The Ag···Ag distances amount to 4.9 Å in **6** and 4.7 Å in **7** suggesting no argentophilic interactions.[11]

Compounds **6** and **7** are well soluble in CH_2Cl_2, THF and CH_3CN, slightly soluble in toluene and insoluble in *n*-pentane. Their room temperature ^{31}P NMR spectra in CD_3CN show singlets centered at -78.5 ppm (**6**) and -79.3 ppm (**7**), which are upfield shifted as compared to that of the free P_2 ligand complex **1** (δ = -43.2 ppm)[10] and downfield shifted compared to the dimeric precursor **2** (δ = -86.1 ppm).[6a] Their room temperature ^1H and $^{13}C\{H\}$ NMR spectra show the expected signals attributed to the proton and carbon nuclei of the ligand complex **1** and the corresponding organic linker (**3** or **4**, for further details see SI). The ^{19}F NMR spectra are featured by characteristic signals for the $[TEF]^-$ counteranion. The ESI mass spectra of **6** and **7** in CH_3CN show peaks in the positive ion mode for the monocations $[Ag\{Cp_2Mo_2(CO)_4P_2\}_2(L)]^+$ (L = **3** or **4**) as well as peaks for smaller fragments indicating a partial dissociation of the CPs **6** and **7** in solutions of CH_3CN. In the negative ion mode, the peak with 100% intensity corresponds to the $[TEF]^-$ anion. The IR spectra of **6** and **7** exhibit each two strong bands at *ca.* $\upsilon_{(CO)} \approx 1920$ and 1980 cm^{-1}, which can be attributed to the carbonyl moieties of **1**.

In a second step, an analogous reaction of the Ag^I dimer **2** was performed using the short rigid linker **5**. When this reaction is carried out at room temperature, a mixture of two types of crystals is obtained: red prisms **8** and orange needles **9** in almost a 1:1 ratio (85% overall yield). These two compounds could be easily sorted out under the microscope because of their different habits and colors: **8** (prisms, red), **9** (needles, orange). Moreover, they could also be separated from each other in solution because of their different solubility. Compound **8** is only well soluble in donor solvents such as CH_3CN, but insoluble in other common organic solvents such CH_2Cl_2, while **9** is well soluble in both CH_3CN and CH_2Cl_2. The $^{31}P\{H\}$ NMR spectra in CD_3CN at room temperature of **8** and **9** show similar broad singlets at -75.9 and -74.7 ppm, respectively, which are almost 30 ppm upfield shifted compared to those of the free P_2 ligand complex **1** and 3 ppm downfield shifted compared to those of the 1D CPs **6** and **7**. These $^{31}P\{H\}$ NMR data suggest only a partial dissociation of the polymers **6**-**9** in CD_3CN, because their complete dissociation to the starting components would show a signal at ca. -43.0 ppm corresponding to the free P_2 ligand complex **1**. The spectroscopic data of **8** and **9** including the ^1H, $^{13}C\{H\}$ and $^{19}F\{H\}$ NMR spectra as well as IR, elemental analysis and mass spectrometry are similar (for further details see SI). Interestingly, the solid state IR spectrum of **8** exhibits one strong band at 1960 cm^{-1} (attributed to the carbonyl groups of the ligand complex **1**) while that of **9** shows two strong bands at 1956 and 2003 cm^{-1}, respectively. These observations suggest that **8** and **9** are similar in solution but different in the solid state with a slight difference in the CO ligands and probably in the coordination modes of their constituting P_2 moieties **1** (constitutional isomers). The X-ray structure analysis performed on single crystals of the two compounds shows that they are indeed structural isomers. Compound **8** is a 2D organometallic-

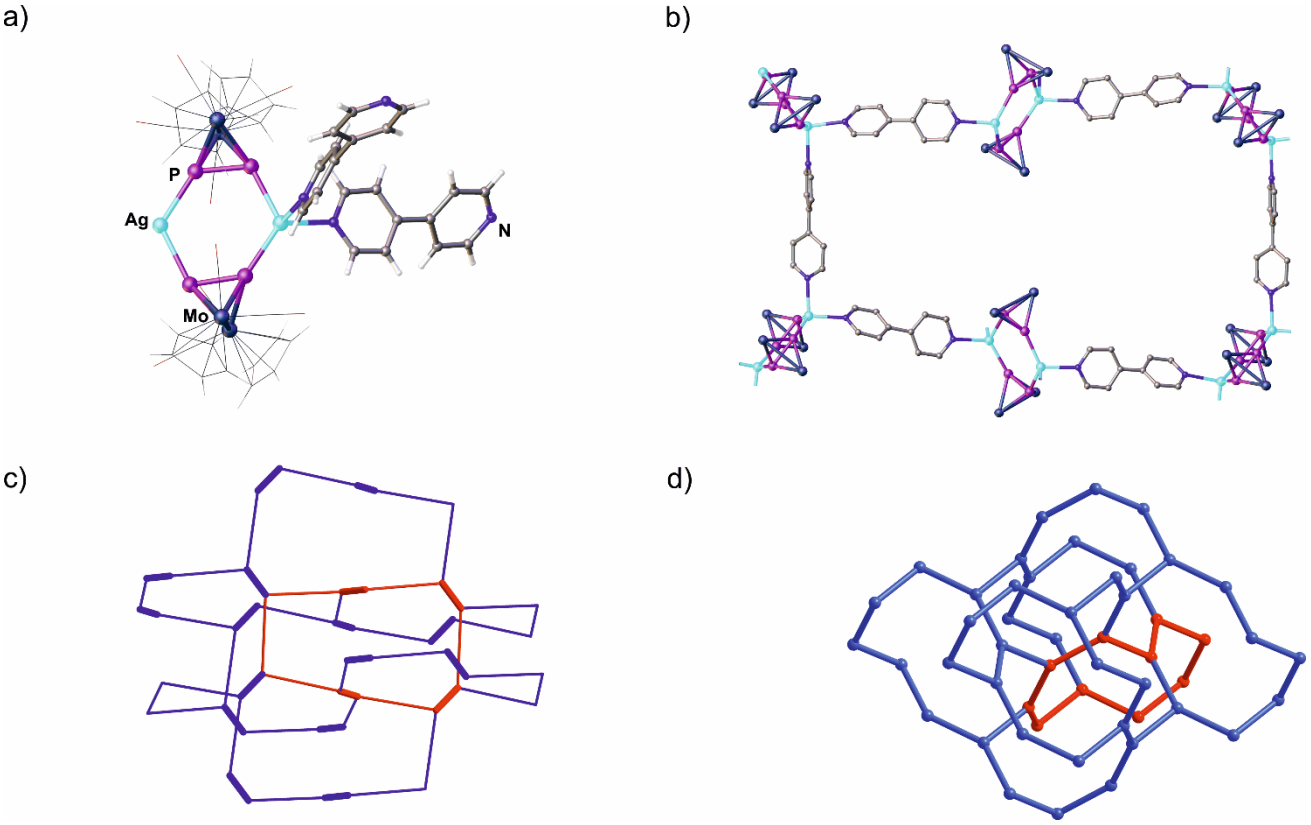

Figure 3. a) The dicationic repeating unit of **9** in the solid state. b) The shortest $Ag_{10}(\mathbf{5})_6\{\mathbf{1}\}_8$ ring. Cp and CO ligands as well as hydrogen atoms are omitted for clarity. c) Section of the simplified **utp** net in **9**[12,13] formed by Ag cations as topological nodes and Mo_2P_2 and bipyridyl ligands as linkers (organic linkers depicted as long rods and $Ag_2P_2(MoCp(CO)_2)_2$ units as thick cylinders). d) Ideal **utp** net. One of the corresponding 10-membered cycles is colored in red in **9** and the ideal **utp**.

organic hybrid polymer while **9** is a 3D organometallic-organic hybrid polymer. In contrast to what was observed in the 1D hybrid CPs **6** and **7**, each of the two polymers **8** and **9** consists of $[Ag_2(\mathbf{1})_2]$ units, which are linked together via the connectors **5** (Figures 2 and 3). Therefore, in the repeating units of **8** and **9**, each of the η^2-coordinated P_2 units presented in the Ag^I dimer **2** is fully substituted by the two pyridyl functions of the two linkers **5**.

In compound **8**, the η^1-η^1 coordinated P_2 ligands present in the Ag^I dimer **2** changed their coordination mode to η^2-η^1-coordination, which is an unusual coordination mode of the P_2 ligand complex.[9e,14] As a consequence, a 2D network is formed where each of the Ag^I ions coordination sphere is occupied by three P atoms, two N atoms and one Ag atom. Organometallic $Ag_2P_2(MoCp(CO)_2)_2$ units form the vertices of the 2D assembly, with cavities having a rhombic shape and a maximum dimension of 1.6 nm.[15] The P-P bond length in **8** (2.123(3) Å) is slightly elongated compared to that of the free P_2 ligand **1** and slightly shortened compared to the 1D CPs **6** and **7**. However, the Ag-P bond lengths (2.592(2)-2.837(2) Å) are longer than those of **6** and **7**. The Ag_2P_4 six-membered rings in the organometallic nodes of **8** are almost planar (folding angle: 6.89°). The Ag···Ag distance is short (2.830 Å) suggesting a possible Ag···Ag interaction.[11]

In contrast to what was observed for the 2D hybrid CP **8**, the η^1-η^1-coordinated P_2 ligands of the Ag^I dimer **2** remain intact in **9**. Each Ag^I ion comprises a distorted tetrahedral geometry with two P atoms and two N atoms. In **9**, organometallic $Ag_2P_2[MoCp(CO)_2]_2$ units form the vertices of a 3D network, with cavities of the meshes having an isosceles trapezoid shape and a maximum dimension of the cavities up to 3.0 nm.[15] The P-P (2.087(2)-2.088(2) Å) and the Ag-P (2.386(4)-2.548(9) Å) bond lengths in **9** are the shortest in the series of all CPs **6**-**9**. Similar to that observed in **8**, the Ag_2P_4 six-membered ring in **9** are almost planar (folding angle: 6.92°). However, the Ag···Ag distance is large (4.543 Å) revealing no Ag···Ag interaction.[11]

For the reaction of the P_2 ligand complex **1** with Ag[TEF] and the short linker **5**, the reason why products (2D + 3D polymers) are afforded differing from those of similar reactions under similar reaction conditions with the longer linkers **3** and **4** is not clear. Most probably, this is due to the steric hindrance between the linker and the pending terminal Mo_2P_2 moiety created during the formation of

the final aggregates upon using the shorter linker. This hindrance is likely to force a full replacement of the two terminal η^2- coordinated P_2 ligands of the intermediate Ag^I dimer **2** with pyridyl functions of the linkers **5** rather than the partial substitution observed when the longer linkers (**3** or **4**) are used.

On the other hand, the reaction with the shortest linker afforded two different products instead of one. Such behavior is mainly related to the difference in the coordination mode of the P_2 ligand complex in the organometallic nodes repeating units leading to a mixture of constitutional isomers (**8** and **9**). As these two compounds crystallized from the same crude reaction mixture, we were interested in investigating the possibility to obtain each of them selectively. For that reason, we performed the same reaction at two different temperatures (0°C and 60°C) keeping all other reaction conditions (dilution, crystallization method, reaction time, etc.) exactly similar. Surprisingly, now these two reactions afforded selective supramolecular aggregations. The reaction at 0°C gave exclusively the 2D hybrid polymer **8**, while the reaction at 60°C allowed the selective formation of the 3D hybrid polymer **9**. All the previous experimental observations suggest that *i)* the CP **9** is probably thermodynamically favored over the CP **8** and *ii)* **8** is an intermediate species isolated during the aggregation reaction to form the 3D hybrid CP **9**.

In order to prove these suggestions, compound **8** was isolated from the reaction at 0°C and dissolved in a 2:1 CH_2Cl_2:CH_3CN mixture. This solution was heated to 60°C, filtered and crystallized by layering with *n*-pentane to yield selectively the 3D CP **9**. DFT calculations were also performed at the B3LYP/def2-TZVP level of theory to investigate the relative stability of the two different coordination modes of **1** found in **8** and **9**. The geometry optimization of the model complex $[Ag_2\{\eta^2,\eta^1\text{-}\{CpMo(CO)_2P_2\}_2\}Py_4]^{2+}$ with the starting geometry derived from the X-ray data of **8** leads to an optimized geometry very similar to that found experimentally in **9**. Fixing the Ag···Ag distance to the value found in the solid state structure of **8** and performing a restrained geometry optimization leads to an optimized geometry that is very similar to the experimental geometry of **8** (η^2,η^1-coordination of **1**). This restrained geometry is with 51.8 $kJ{\cdot}mol^{-1}$ higher in energy than the relaxed one (η^2,η^1 vs. η^2,η^1 coordination). This clearly shows that the η^1-η^1 coordination mode is thermodynamically favored and indicates that **8** represents a kinetic product, while **9** is the thermodynamic one.

Conclusions

In conclusion, we have shown that the three-component reaction using the P_2 ligand complex $[Cp_2Mo_2(CO)_4(\eta^2\text{-}P_2)]$ (**1**) with $Ag[Al\{OC(CF_3)_3\}_4]$ and the rigid bipyridyl linkers **3**-**5** afforded the selective aggregation products **6**-**9** out of a large combination of the starting components. For the first time in this field, we have traced the influence of the ligand size on this supramolecular assembly reaction. Upon using the long linkers **3** and **4**, only 1D hybrid polymers are formed, while by using the shorter linker **5**, a mixture of both 2D (**8**) and 3D (**9**) hybrid polymers is obtained. Moreover, we have demonstrated the influence of the temperature that proved to be crucial for the selective reaction synthesis of **8** or **9**. When performing the reaction at 0°C, only compound **8** is isolated in the solid state, whereas the reaction at 60°C affords **9** as the only accessible product. This is further supported by DFT calculations that show that **9** represents the thermodynamic product of the reaction. Current investigations in this field focus on optimising reaction conditions mainly using longer linkers and smaller anions to create porosity in the formed hybrid CPs for potential application as gas storage materials.

CCDC 1864891, 1864892, 1864893 and 1864894 for **6**-**9** contain the supplementary crystallographic data for this paper. These data can be obtained free of charge from The Cambridge Crystallographic Data Center.

Acknowledgements

The authors gratefully acknowledge the European Research Council for the Grant ERC-2013-AdG339072 for the financial support of this work. Parts of this research were carried out at PETRA III at DESY, a member of the Helmholtz Association (HGF). We would like to thank Dr. S. Panneerselvam, Dr. B. Dittrich and Dr. A. Burkhardt for their assistance regarding the use of the beamline P11 (research project I-20160654).

Conflicts of interest

There are no conflicts to declare.

Notes and references

1 a) J.-W. Cui, S.-X. Hou, K. V. Hecke and G.-H. Cui, *Dalton Trans*, 2017, **46**, 2892; b) X.-Y. Dong, C.-D. Si, Y. Fan, D.-C. Hu, X.-Q. Yao, Y.-X. Yang and J.-C. Liu, *Cryst. Growth Des.*, 2016, **16**, 2062; c) X. Zhang, W. Wang, Z. Hu, G. Wang and K. Uvdal, *Coord. Chem. Rev.* 2015, **284**, 206; d) C. He, D. Liu and W. Lin, *Chem. Rev.* 2015, **115**, 11079; e) L. Carlucci, G. Ciani, D. M. Proserpio, T. G. Mitina and V. A. Blatov, *Chem. Rev.* 2014, **114**, 7557; f) J. Heine and K.-M. Buschbaum, *Chem. Soc. Rev.* 2013, **42**, 9232; g) W. L. Leong and J. J. Vittal, *Chem. Rev.* 2011, **111**, 688.

2 a) T. R. Cook, Y.-R. Zheng and P. J. Stang, *Chem. Rev.* 2013, **113**, 734; b) S Park, S. Y. Lee, K.-M. Park and S. S. Lee, *Acc. Chem. Res.* 2012, **3**, 391; c) R. Chakrabarty, P. S. Mukherjee and P. J. Stang, *Chem. Rev.* 2011, **11**, 6810; d) F. A. Cotton, E. V. Dikarev and M. A. Petrukhina, *Angew. Chem. Int. Ed.* 2001, **40**, 1521.

3 a) R. S. Patil, A. M. Drachnik, H. Kumari, C. L. Barnes, C. A. Deakyne and J. L. Atwood, *Cryst. Growth Des*. 2015, **15**, 2781; b) B. Liu, N. Li, W.-P. Wu, H. Miao, Y.-Y. Wang and Q.-Z. Shi, *Cryst. Growth Des*. 2014, **14**, 1110; c) K. P. Rao, M. Higuchi, J. Duan and S. Kitagawa, *Cryst. Growth Des*. 2013, **13**, 981; d) C.-P. Li, J.-M. Wu and M. Du, *Chem. Eur. J.* 2012, **18**, 12437; e) H. J. Park and M. P. Suh, *CrystEngComm*, 2012, **14**, 2748; f) K. Tripuramallu, P. Manna and S. K. Das, *CrystEngComm*, 2014, **16**, 4816; g) R.-J. Wei, J. Tao, R.-B. Huang and L.-S. Zheng, *Eur. J. Inorg. Chem*. 2013, **5-6**, 916; h) H. T. Chifotides, I. D. Giles and K. R. Dunbar, *J. Am. Chem. Soc.,* 2013, **135**, 3039; d) F.-J. Liu, D. Sun, H.-J. Hao, R.-B. Huang and L.-S. Zheng, *Cryst. Growth Des*. 2012, **12**, 354.

4 a) M. El Sayed Moussa, S. Evariste, H.-L. Wong, L. Le Bras, C. Roiland, L. Le Polles, K. Costuas. V. W.-W. Yam and C. Lescop, *Chem. Commun*., 2016, **52**, 11370; b) G. Dura, M. C. Carrion, F. A. Jalon, B. R. Manzano, A. M. Rodriguez and K. Mereiter, *Cryst. Growth Des.* 2015, **15**, 3321; c) J.-Z. Gu, Y.-H. Cui, J. Wu,

A. M. Kirillov and *RSC. Adv*. 2015, **96**, 78889; d) J.-M. Hao, B. Y. Yu, K. V. Hecke and G.-H. Cui, *CrystEngComm*. 2015, **17**, 2279; e) G. Kumar and R. Gupta, *Chem. Soc. Rev*. 2013, **42**, 9403; f) S. Wang, T. Zhao, G. Li, L. Wojtas, Q. Huo, M. Eddaoudi and Y. Liu, *J. Am. Chem. Soc*., 2010, **132**, 18038; g) B. Nohra, Y. Yao, C. Lescop and R. Réau, *Angew. Chem., Int. Ed*., 2007, **46**, 8242; h) Z. Qin, M. C. Jennings and R. J. Puddephatt, *Chem. Eur. J.* 2002, **8**, 735; i) M. J. Irwin, J. J. Vittal, G. P. Yap and R. J. Puddephatt, *J. Am. Chem. Soc*. 1996, **118**, 13101; j) F. A. Cotton, C. Lin and C. A. Murillo, *Proc. Natl. Acad. Sci*. U.S.A. 2002, **99**, 4810; k) F. A. Cotton, C. Lin and C. A. Murillo. *Acc. Chem. Res*. 2001, **10**, 759.

5 a) H.-N. Wang, G.-G. Shan, H.-B. Li, X.-L. Wang, H.-T. Cao and Z.-M. Su, *CrystEngComm*, 2014, **16**, 2754; b) A. N. Khlobystov, A. J. Blake, N. R. Champness, D. A. Lemenovskii, A. G. Majouqa, N. V. Zyk and M. Schröder, *Coord. Chem. Rev*., 2001, **222**, 155; c) M. Fujita, K. Umemoto, M. Yoshizawa, N. Fujita, T. Kusukawa and K. Biradha, *Chem. Commun*., 2001, **6**, 509; d) B. J. Holliday, C. A. Mirkin, *Angew. Chem., Int. Ed*., 2001, **40**, 2022.

6 a) M. E. Moussa, M. Fleishmann, E. V. Peresypkina, L. Dütsch, M. Seidl, G. Balázs and M. Scheer, *Eur. J. Inorg. Chem*., 2017, **25**, 3222; b) C. Heindl, A. Kuntz, E. V. Peresypkina, A. V. Virovets, M. Zabel, D. Lüdeker, G. Brunklaus and M. Scheer, *Dalton Trans*., 2015, **44**, 6502; c) C. Heindl, E. V. Peresypkina, A. V. Virovets, V. Y. Komarov and M. Scheer, *Dalton Trans*., 2015, **44**, 10245; d) M. Fleishmann, S. Welsch, E. V. Peresypkina, A. V. Virovets and M. Scheer, *Chem. Eur. J.* 2015, **21**, 14332; e) F. Dielmann, C. Heindl, F. Hastreiter, E. V. Peresypkina, A. V. Virovets, R. M. Gschwind and M. Scheer, *Angew. Chem. Int. Ed*. 2014, **53**, 13605; f) E.-M. Rummel, M. Eckhardt, M. Bodensteiner, E. V. Peresypkina, W. Kremer, C. Gröger and M. Scheer, *Eur. J. Inorg. Chem*. 2014, **10**, 1625; g) H. Krauss, G. Balázs, M. Bodensteiner and M. Scheer, *Chem. Sci*., 2010, **1**, 337; h) M. Scheer, L. J. Gregoriades, A. V. Virovets, W. Kunz, R. Neueder and I. Krossing, *Angew. Chem. Int. Ed*. 2006, **45**, 5689; i) J. Bai, A. V. Virovets and M. Scheer, *Angew. Chem. Int. Ed*. 2002, **41**, 1737.

7 a) C. Heindl, E. Peresypkina, A. V. Virovets, I. S. Bushmarinov, M. G. Medvedev, B. Krämer, B. Dittrich and M. Scheer, *Angew. Chem. Int. Ed*. 2017, **43**, 13237; b) E. Peresypkina, C. Heindl, A. Virovets and M. Scheer. Inorganic Superspheres. In: Dehnen S. (eds) Clusters – Contemporary Insight in Structure and Bonding. *Structure and Bonding* 2016, **174**, 321; c) C. Heindl, E. V. Peresypkina, D. Lüdeker, G. Brunklaus, A. V. Virovets and M. Scheer, *Chem. Eur. J.* 2016, **22**, 2599; d) C. Heindl, E. V. Peresypkina, A. V. Virovets, W. Kremer and M. Scheer, *J. Am. Chem. Soc.* 2015, **137**, 10938; e) M. Fleischmann, S. Welsch, H. Krauss, M. Schmidt, M. Bodensteiner, E. V. Peresypkina, M. Sierka, C. Gröger and M. Scheer, *Chem. Eur. J.* **2014**, *20*, 3759; e) F. Dielmann, C. Heindl, F. Hastreiter, E. V. Peresypkina, A. V. Virovets, R. M. Gschwind and M. Scheer, *Angew. Chem. Int. Ed.* 2014, **53**, 13605; f) M. Scheer, A. Schindler, R. Merkle, B. P. Johnson, M. Linseis, R. Winter, C. E. Anson and A. V. Virovets, *J. Am. Chem. Soc.* 2007, **129**, 13386; g) J. Bai, A. V. Virovets and M. Scheer, *Science* 2003, **300**, 781.

8 S. Welsch, C. Groeger, M. Sierka and M. Scheer, *Angew. Chem. Int. Ed.* 2011, **50**, 1435.

9 a) M. E. Moussa, S. Welsch, L. J. Gregoriades, G. Balázs, M. Seidl and M. Scheer, *Eur. J. Inorg. Chem*. 2018, 1683; b) M. E. Moussa, B. Attenberger, E. V. Peresypkina and M. Scheer, *Dalton Trans.,* 2018, **47**; 1014; c) M. E. Moussa, B. Attenberger, M. Seidl, A. Schreiner and M. Scheer, *Eur. J. Inorg. Chem*. 2017, **47**, 5616; d) M. E. Moussa, M. Seidl, G. Balazs, A. V. Virovets, B. Attenberger, A. Schreiner and M. Scheer, *Chem. Eur. J*. 2017, **23**, 16199; e) M. E. Moussa, B. Attenberger, M. Fleischmann, A. Schreiner and M. Scheer, *Eur. J. Inorg. Chem*. 2016, **28**, 4538; f) M. Elsayed Moussa, B. Attenberger, E. V. Peresypkina, M. Fleischmann, G. Balázs and M. Scheer, *Chem. Commun*. 2016, **52**, 10004; g) B. Attenberger, E. V. Peresypkina and M. Scheer, *Inorg. Chem.* 2015, **54**, 7021; h) B. Attenberger, S. Welsch, M. Zabel, E. Peresypkina and M. Scheer, *Angew. Chem. Int. Ed*., 2011, **50**, 11516.

10 M. Scheer, L. J. Gregoriades, M. Zabel, J. Bai, I. Krossing, G. Brunklaus and H. Eckert. *Chem. Eur. J*. 2008, **14**, 282.

11 H. Schmidbaur and A. Schier, *Angew. Chem. Int. Ed*. 2015, **54**, 746.

12 a) Topological type according to Reticular Chemistry Structure Resource database, M. O'Keeffe, M. A. Peskov, S. J. Ramsden and O. M. Yaghi, *Accts. Chem. Res.* 2008, **41**, 1782; b) M. O'Keeffe, M. Eddaoudi, H. Li, T. Reineke and O. M. Yaghi, *J. Solid State Chem.* 2000, **152**, 3. http://rcsr.net/nets/ths

13 According to the information from the *ToposPro* programm; V. A. Blatov, A. P. Shevchenko and D. M. Proserpio, *Cryst. Growth & Des*. 2014, **14**, 3576.

14 S. Welsch, C. Lescop, G. Balazs, R. Reau and M. Scheer, *Chem. Eur. J.* 2011,**17**, 9130.

15 Calculated as the diagonal distances between Ag^+ ions minus the doubled ionic radius of Ag^+ ions for the coordination number 4 (1.14 Å).